Hindawi
Geofluids
Volume 2022, Article ID 2332743, 12 pages
https://doi.org/10.1155/2022/2332743

Research Article

Mechanism of Filtration Behaviors of Cement-Based Grout in Saturated Sand under Different Grouting Conditions

Shanlin Xu, Hongtao Cao, Yanzhen Zhu, Honglei Sun, Jingling Lu, and Junqiang Shi

College of Civil Engineering, Zhejiang University of Technology, Hangzhou, Zhejiang 310023, China

Correspondence should be addressed to Honglei Sun; sunhonglei@zju.edu.cn

Received 21 January 2022; Accepted 31 March 2022; Published 5 May 2022

Academic Editor: Xueming Du

Cement-based grout has been widely used in various civil engineering applications. However, the filtration behaviors of it when grouting the porous geological masses vary a lot under different grouting conditions, which significantly influences its penetration and the enhancement effect. The purpose of this work was to better understand the filtration of cement-based grout in porous sand by conducting a series of visualized laboratory tests and EDTA titration tests. The experimental results show that the cement filtration, including the penetration, retention, and formation of cement filter cake above the grouting body, is collectively influenced by different grouting factors. With the increase of the soil samples' pore size and the cement slurry's water-cement ratio, the penetrated distance and amount of cement in sand increase. However, the penetration does not increase monotonically with the grouting pressure. Too excessive grouting pressure (e.g., 300 kPa in this study) accelerates the formation of cement filter cake and thus stops the subsequent cement infiltration. The mechanisms of different filtration behaviors were explained from microscopic particle clogging in the pore throat of the porous media. Furthermore, the reduced permeability of the sand column with the retained cement due to filtration was discussed, and the dewatering phenomenon of the cement slurry after filter cake formation was first revealed.

1. Introduction

Grouting is widely used in geotechnical applications, including sealing tunnels and underground excavations, reducing or stopping water inflow, and enhancing the fractured rock and soil [1–3]. At present, there are mainly two types of materials used for grouting reinforcement, e.g., cement-based grout and chemical grout. As the cement-based grout has a low environmental impact and affordable cost, it is extensively utilized in numerous civil engineering applications [4–7]. However, with the cement suspensions (cement slurry) seeping into the grouting body, the solid cement particles are retained by the pore throat of porous media at different locations (called filtration effect [8]). The void ratio of the porous grouting body decreases significantly due to the filtration, reducing the cement's infiltration (penetration) and influencing the enhancement effect. Thus, much experimental and analytical research has been conducted to investigate the filtration effect of cement and its deciding factors.

Herzig et al. [8] proposed that the filtration of the suspensions through porous media is related to various factors, namely, the carrier fluid (including flow rate, viscosity), the suspensions of particles (e.g., concentration, particle size), and the porous medium filter (porosity, pore size). Xu and Bezuijen [1] studied the bentonite slurry penetration in front of the slurry TBM. They proposed two stages of penetration: mud spurt and filter cake formation. Additionally, they indicated that the theoretically maximum penetration distance estimated by the well-known penetration distance function proposed by Krause [9] and Broere [10] is much greater than the measured value, as the filtration is not considered accurately. Yousif et al. [11] discussed the effect of pore levels on physical plugging and proposed the value of the reduced permeability after plugging is proportional to the square of D_{15} of the porous media and d_{85} of suspensions. Ma et al. [12, 13] studied the non-Darcy hydraulic properties, deformation behaviors, and failure patterns of rock in underground mining. Zhou et al. [14] studied the effect of

different grouting methods, i.e., constant flow rate and constant pressure, on the penetration of cement slurry and proposed that the excessive grouting rate or pressure is not conducive to the penetration. Additionally, the water-cement ratio (W/C ratio), defined as the weight ratio between water and cement in the cementitious mix, is a critical grouting factor that determines both the carrier fluid's viscosity and the solid particle concentration. Axelsson et al. [15] discussed the influence of the water-cement ratio (W/C = 1 ~ 3) on the sand's penetrability and proposed that the higher water-to-cement ratios result in a larger penetration area. Additionally, the water-cement ratio and the pore size of the porous media collectively determine the cement penetration.

Previous research has shown that the filtration behaviors of cement-based grouts differ considerably under different grouting conditions, which are influenced by the pore size of porous media, the water-cement ratio, and the grouting rate or pressure simultaneously. However, the mechanisms of different filtration behaviors remain unclear, and the coupled effects of these grouting conditions are not well understood. In addition, in previous studies about saturated sand column grouting, the water-cement ratio of the grouting materials was typically greater than 1. The study of the low W/C-ratio grout in saturated sand, which is a common grouting condition for the backfill grouting for shield tunnels, is rare. Therefore, the purpose of the present work is to better understand how the abovementioned grouting factors influence the filtration behaviors under low W/C ratio grouting conditions and discuss the filtration mechanisms from a microscopic view of particle clogging.

To predict the slurry penetration process in most numerical or analytical studies (Herzig et al. [8], Bouchelaghem and Vulliet [16], Saada et al. [17], Kim and Whittle [18], and Zhou et al. [19]), the variation of the grouting body's porosity and the permeability due to filtration is critical for both constructing the theoretical equations and determining the value of filtration-relevant coefficients. The measurement of the penetrated cement content is fundamental to understand the filtration and predict the grout penetration in porous media. However, for sand samples, the loose packing structure increases the difficulties and inaccuracy of the cement content's measurement at different depths. Recently, Li et al. [5] studied the dispersion of cement grout in sand through the Ethylenediaminetetraacetic Acid (EDTA) titration test. As this method could obtain the accurate cement content from loose sand samples, it was utilized in this work to study the distribution of the penetrated cement content in the soil after grouting.

By conducting a series of visualized laboratory tests and EDTA titration tests, the development of the cement's penetrated distance and content in the sand under different grouting conditions was systematically analyzed. The main aim of the paper is to investigate the following key questions:

(1) To evaluate the effect of the pore size of the soil column, water-cement ratio, and grouting pressure on cement filtration in saturated sand. And the turning points of different conditions were analyzed

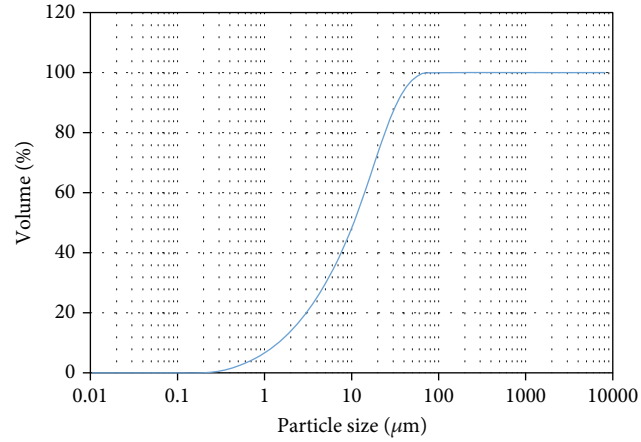

Figure 1: The particle size distribution of the P.O42.5 Portland cement.

(2) To calculate the contribution of cement content due to the filtration on the permeability coefficient of saturated sand column

(3) To explain the mechanism of the cement filtration in the grouting body and the formation of the cement filter cake above the grouting body

2. Materials and Methods

2.1. Materials. The grouting material used in this study is P.O42.5 Portland cement, and its grading curve is shown in Figure 1. The particle size distribution of the cement particles was obtained by the laser particle size analyzer; and ethanol was used as the dispersing solvent to avoid the hydration reaction of the cement slurry. The DV3T rotational rheometer was utilized to acquire the viscosity and access the rheological properties of slurries with different water-cement ratios (see Figure 2).

Three kinds of sand samples with different particle size ranges were utilized as the grouting body, named fine sand (0.1-0.5 mm), medium sand (0.25-1.2 mm), and coarse sand (0.5-5 mm), in the study. The grading curves of these three sand samples are shown in Figure 3. The parameters of these three sand samples are shown in Table 1.

2.2. Methods

2.2.1. Grouting Tests. A fully saturated sand column was grouted based on the self-developed transparent one-dimensional grouting device (see Figures 4 and 5). Before the grouting, the grouting barrel was filled with air, cement slurry, saturated sand, filter paper, and porous stone from top to bottom. In the grouting stage, the air compressor was connected to the upper vent of the grouting barrel to provide the constant grouting pressure. A pressure regulating valve was used for constant pressure control. The lower vent of the grouting barrel was connected to a bucket where the water with a free surface was stored. The water level in the bucket was always controlled at the same height as the saturated sand column to provide the conditions of pressure-

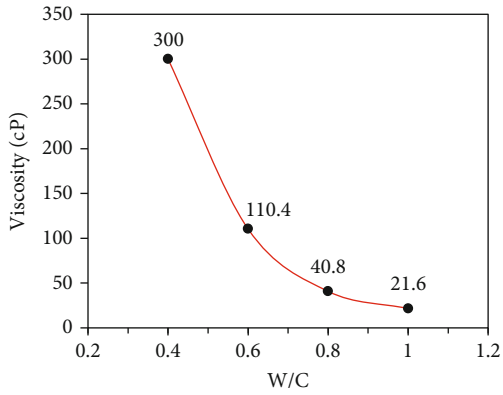

Figure 2: The viscosity of cement grout with different water-cement ratios.

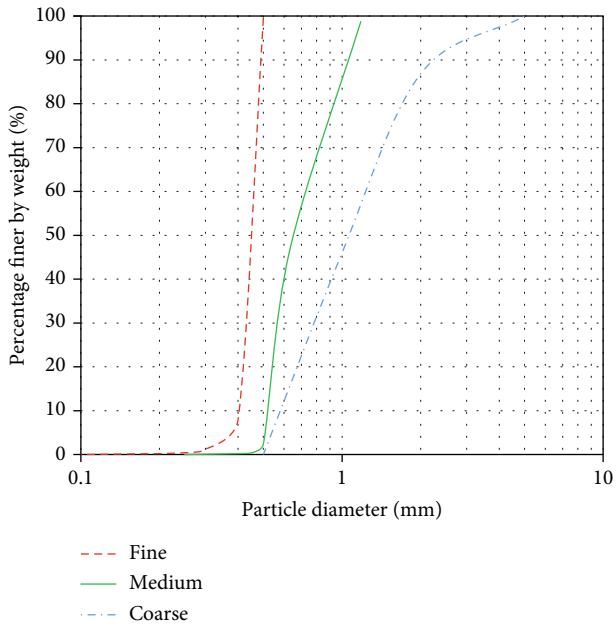

Figure 3: The grading curves of three sand samples.

limited drainage of the actual grouted soil. The grouting time under constant pressure is set as 3 min. We monitored and recorded the real-time penetration (or diffusion) of the cement slurry into the sand column during the grouting. After grouting, the cement-sand mixed specimens were sampled in layers (the thickness of all samples is 1 cm, and a total of 10 were taken). The EDTA (the Ethylenediaminetetraacetic Acid) titration method was used to determine the cement content at different depths of the infiltration into the soil column.

In this experiment, the effects of three factors, namely, the averaged pore size of sand samples, water-cement ratio of cement slurry, and the value of constant grouting pressure, on the filtration effect were studied separately. The details of the grouting tests are shown in Table 2. Tests 1, 2, and 3 used three kinds of sand samples with different particle size ranges of 0.1-0.5 mm, 0.25-1.2 mm, and 0.5-5.0 mm. Tests 4, 2, 5, and 6 utilized cement slurry with different water-cement ratios of 0.4, 0.6, 0.8, and 1.0 for grouting. The cement slurry was both prepared with a vertical mixer. The mixing time is 20 min, and the mixing speed keeps constant with the value of 1000 r/min. The grouting pressure used in tests 7, 2, 8, and 9 is 100, 200, 300, and 400 kPa. The experimental setups of different grouting tests were set based on a backfill grouting project for the shield tunnel.

Table 1: Parameters for sand samples in the study.

Sand	Nonuniformity coefficient	Coefficient of curvature	Relative compactness
Coarse	2.02	0.84	0.72
Medium	1.44	0.80	0.70
Fine	1.15	1.00	0.66

2.2.2. EDTA Titration Tests. This work used the EDTA titration method to determine the cement content in grouted soil samples. We first obtained the EDTA titration curve that indicates the relationship between the cement content of sand samples and the titration amount of disodium EDTA solution by calibration test. Six kinds of samples were prepared in advance, that is, 100 g of saturated sand samples with the cement content of 0%, 2%, 4%, 6%, 8%, and 10%, respectively. After leaving the prepared mixed samples to hydrate for 1 h, we put them into a 105°C oven for 12 h. After this, the dried samples were taken out, ground, and poured into a 500 ml beaker, and then added an appropriate amount of weak acid solvent, 10% NH_4Cl solution. After dissolving Ca^{2+} with sufficient stirring, left them for 3 h. A large amount of Ca^{2+} ions and a small amount of Fe^{3+}, Al^{3+}, etc. were left in the solution. The following is the chemical formula of this process:

$$Ca(OH)_2 + NH_4Cl = CaCl_2 + 2NH_3 \cdot H_2O \quad (1)$$

Subsequently, 10 ml of the clear upper solution was pipetted into a 200 ml conical flask, and 50 ml of 1.8% NaOH solution and 2 ml triethanolamine were added, adjusting the pH of the solution to be greater than 12.5. In the alkaline environment, triethanolamine made Fe^{3+}, Al^{3+} and a small amount of Mg^{2+}, Mn^{2+} form a precipitate, so the reaction between the disodium EDTA standard solution and Ca^{2+} was not interfered. Then, 0.2 g of calconcarboxylic acid indicator was added to the filtrate, and the filtrate was shaken well to form a red chromium complex of Ca^{2+}. Later, the filtrate was titrated with 0.1 mol/m^3 of disodium EDTA standard solution and kept shaking. The chemical formula for the reaction occurring in the mixture is as follows:

$$\begin{aligned} &Ca^2{+}{+}Xn^{2-} \_\_\_\_\_ CaX_n(\text{rose}) \\ &Ca^{2+} + Y^2 - \_\_\_\_\_ CaY(\text{colorless}) \\ &CaX_n + Y^{2-} \_\_\_\_ CaY(\text{colorless}) + Xn^{2-}(\text{solid blue}) \end{aligned} \quad (2)$$

where $X_n{}^{2-}$ stands for the anions involved in the reaction in the calconcarboxylic acid indicator, and Y^{2-} represents the anions involved in the reaction in EDTA disodium.

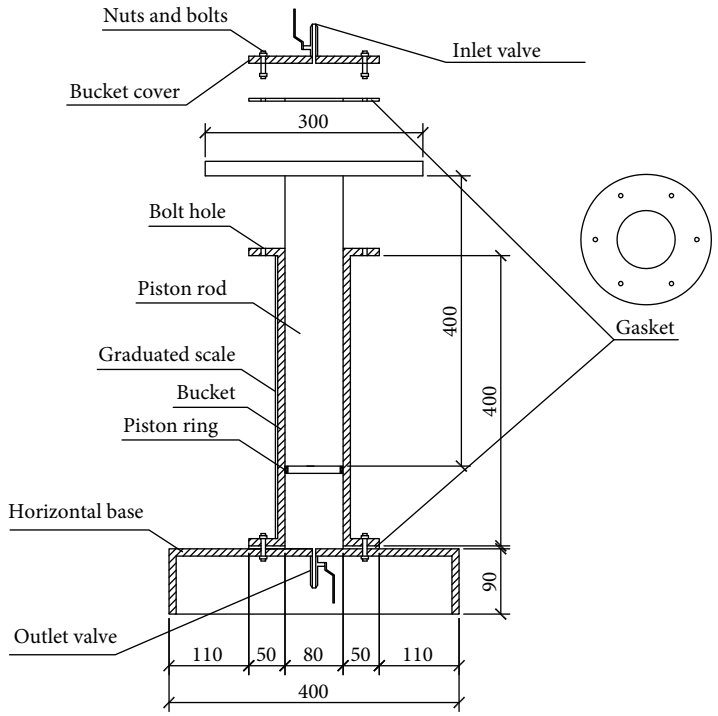

Figure 4: Grouting device.

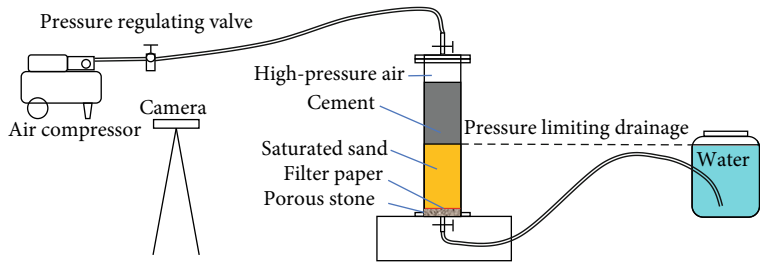

(a) Schematic diagram of the grouting process

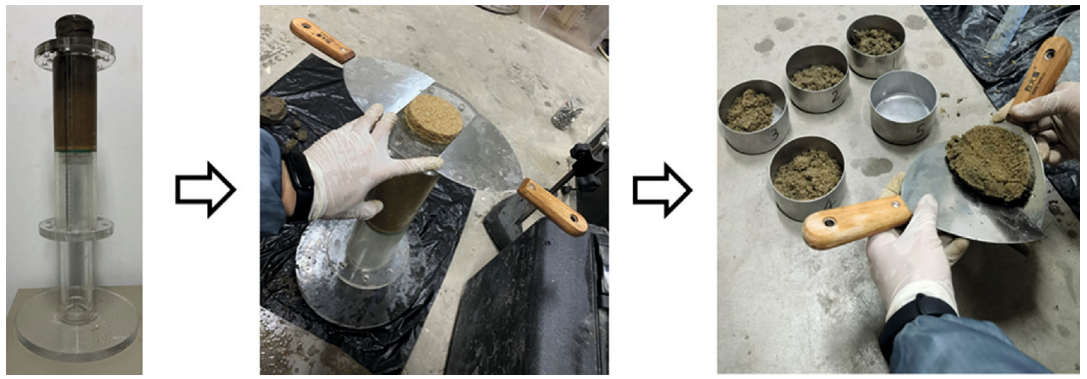

(b) Photos of sampling process

Figure 5: Grouting and sampling methods.

In the solution with pH greater than 12.5, Y^{2-} is easy to combine with Ca^{2+}, forming a colorless chromium complex CaY, which is more stable than the chromium complex Ca X_n formed by the $X_n{}^{2-}$ and Ca^{2+}. Therefore, when the C a^{2+} solution in the presence of calconcarboxylic acid dropped into the standard solution of EDTA disodium, the EDTA disodium would take away Ca^{2+} in CaX_n (rose complex) and make the calconcarboxylic acid $X_n{}^{2-}$ free out. When the rose complex is completely consumed, the mixed solution changes to its original color of calconcarboxylic acid, which is solid blue (see Figure 6). This titration amount is the consumption of EDTA disodium titration amount

Table 2: Parameters for grouting experiments.

No. of tests	Influencing factor 1 Particle size range (mm)	Influencing factor 2 W/C	Influencing factor 3 Grouting pressure (kPa)
1	0.1-0.5	0.6	200
2	0.25-1.2	0.6	200
3	0.5-5.0	0.6	200
4	0.25-1.2	0.4	200
5	0.25-1.2	0.8	200
6	0.25-1.2	1	200
7	0.25-1.2	0.6	100
8	0.25-1.2	0.6	300
9	0.25-1.2	0.6	400

corresponding to the cement content of saturated sand samples.

For each type of soil (with different particle sizes), we conducted titrations on six kinds of samples with different cement contents (each was titrated twice) to obtain titration curves. The expressions of the titration curve for soil samples were determined by linear fitting, as shown in Figure 7 and Table 3.

3. Results

3.1. Penetration Variation of the Cement Slurry in the Soil Column. The penetration of the cement slurry in the sand column can be observed through the transparent cylindrical column. Based on EDTA test results, the observed farthest penetration surface has the cement content of 2.8%. The variations of the penetration with time under different grouting conditions are shown in Figures 8–10. The solid lines in these figures indicate the location of the farthest penetration surface of the slurry, and the dashed lines represent the location of the top surface of the cement slurry (interface between the slurry and the air). The initial penetration distance of the slurry at $t = 0$ s before grouting is not zero because the slurry seeps and diffuses in porous sand due to gravity. As shown in Figure 8, the initial penetration rate is high under the constant grouting pressure and then gradually decreases. Gradually, the penetration in soil will no longer increase under grouting. It is because, with the development of the filtration (retention) of cement, the retained cement reduces the injectability and the permeability of the soil column, resulting in a decrease or stoppage of subsequent cement penetration. After the penetrated slurry stabilizes, the top surface of the cement slurry still varies slowly. It indicates that the cement filter cake forms above the soil column (discussed in Section 4.3) stops cement particles' injecting but allows the water in cement-slurry passing through. The cement is dewatered instead of penetrating the soil under pressure. This study defines the maximum stable penetration length as the maximum slurry penetration distance. By comparing the slurry penetration in different sand columns, the cement slurry penetrates faster in coarse-grained sand columns, with a larger maximum penetration distance and a longer time to reach the maximum penetration.

Figure 9 demonstrates the effect of grouting pressure on the penetration. As the grouting pressure is in the range of 100-300 kPa, the slurry penetration rate and the maximum penetration distance increase with the growth of the grouting pressure. However, when the slurry develops from 300 kPa to 400 kPa, the slurry penetration rate and maximum penetration distance decrease. The maximum penetration distance of the slurry under the constant pressure of 100-400 kPa is 27 mm, 36 mm, 44 mm, and 38 mm, respectively. This study's maximum penetration occurs at a grouting pressure of 300 kPa. Since the maximum penetration distance is not always positively correlated with the grouting pressure, the enhancement effect in practical grouting projects does not increase continuously with the growth of the grouting pressure. In some grouting conditions (where particles are blocked and a filter cake forms), too high grouting pressure will aggravate cement filtration and reduce cement penetration.

As shown in Figure 10, with the growth of the water-cement ratio, the cement slurry penetration rate and the maximum penetration distance increase, and the time to reach the maximum penetration distance is delayed. It is noteworthy that in all of our grouting tests, the cement top surface continues to decrease after penetration has stabilized. It implies that the cement filter cake forms above the soil column (discussed in Section 4.1) in all grouting tests.

3.2. The Penetrated Cement Content and Total Injected Amount in the Soil Column. From Figure 11, the penetrated cement content increases with the growth of the particle sizes of the sand column. The larger the sand particle size is, the larger the averaged pore sizes of the saturated sand column will be. The cement particles are less likely to be retained, and more cement particles can be injected and penetrate soil. However, with the increase of grouting pressure, the penetrated cement content in the soil exhibits a trend of increasing first and then decreasing (see Figure 12). When the grouting pressure increases from 100 kPa to 300 kPa, the cement contents at different depths increase with the growth of the grouting pressure. However, the cement content decreases as the grouting pressure increases from 300 kPa to 400 kPa. It is because the excessive grouting pressure results in a significant filtration effect. The cement filter cake that prevents the subsequent cement particles from penetrating soil forms more quickly at the higher grouting pressure.

Additionally, as is shown in Figure 13, the penetrated cement contents in the soil increase with the development of the cement slurry's water-cement ratio. The viscosity of cement slurry decreases as the water-cement ratio increases (see Figure 2). Thus, the slurry with the greater water-cement ratio can be injected into soil at a higher rate under the same grouting pressure. In addition, the cement particle clogging decreases as the solid volume concentration of the high-water-cement slurry is lower (as discussed in Section 4.1), thus the penetration increases. However, when the water-cement ratio is greater than 0.8 in this work, the

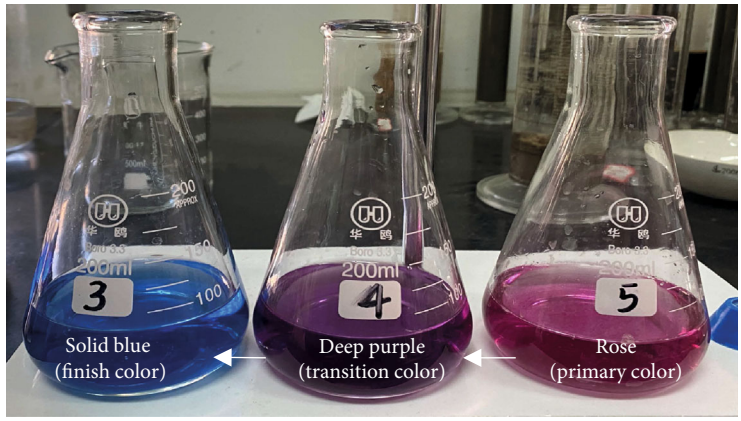

Figure 6: Colors of titrated solution.

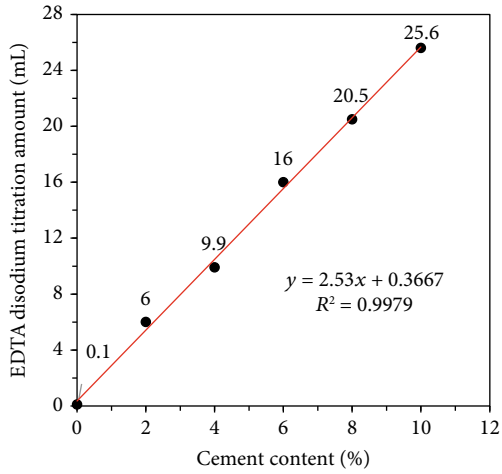

Figure 7: Correlation between cement content in medium sand and EDTA disodium titration amount.

increase of cement penetration with the growth of the water-cement ratio is not significant. It is inferred that the injected cement particle concentration decreases with the increase of the water-cement ratio, and thus, the solid cement content in the soil does not increase significantly.

The total penetrated amounts of cement in the soil column under different grouting conditions are calculated based on the distribution of cement content in the soil column. According to Axelsson et al. [15], the ratio between the cement grain size and the available opening of the pores is critical to assess the extent of cement's stoppage. In this work, the size of the available opening is calculated by hydraulic measuring method based on Kozeny-Carmans equation [19] and Axelsson et al. [15], as shown below:

$$b_{K-C} = \frac{n}{(1-n)\cdot S_0}\cdot\sqrt{12\cdot C_3}, \quad (3)$$

where n is the porosity of the soil column, measured during the experiments (see Table 4). S_0 represents the specific surface area, determined from the grain distribution curves (see Figure 1). v is the fluid's kinematic viscosity, and C_3 represents the shape factor constant that is set as 0.2 for spherical grains according to Carman [20], who conducted an extensive literature survey and concluded that this value is relatively constant for spherical grains. Additionally, the size ratio of the opening to the d_{90} of cement particle b_{K-C}/d_{90} can be obtained, as shown in Table 4.

Table 3: Calibration curve of EDTA titration method in the study.

Size	Rating curve	R^2
Coarse sand	$y = 2.4129x + 1.919$	0.9722
Medium sand	$y = 2.53x + 0.3667$	0.9979
Fine sand	$y = 2.6314x + 0.2095$	0.9948

The relationship between the b_{K-C}/d_{90} and the total amount of injected cement is shown in Figure 14. With the increase of the value of b_{K-C}/d_{90}, the penetrability of the soil is greater, and thus, more cement particles are penetrated the soil column. The relationship between the water-cement ratio and the total amount of injected cement is also presented. From Figure 15, the total cement amount positively correlates to the water-cement ratio. Nevertheless, when the water-cement ratio is greater than 0.8, the solid grouting amount no longer increases with the improvement of the water-cement ratio. As for the grouting pressure, with the increase of the grouting pressure, the total amount of cement injection is positively correlated with the grouting pressure when pressure is lower than 300 kPa (see Figure 16). With the further increase of the pressure, the total amount of cement penetration decreases due to the cement filter cake forming more quickly. The cement particles could not be injected into the soil after the formation of cement filter cake, which will be discussed in Section 4.1.

4. Discussion

4.1. Mechanism of Filtration Effects from the View of Particle Clogging in the Pore Throat. From a microscopic view, when cement particles pass through porous media, they can clog or get stuck in the pore throats (openings) of the porous media (filtration). The particle clogging in the pore throats could be classified as two types (see Figure 17): (a) interception, as the cement particle is larger than the pore throat; (b)

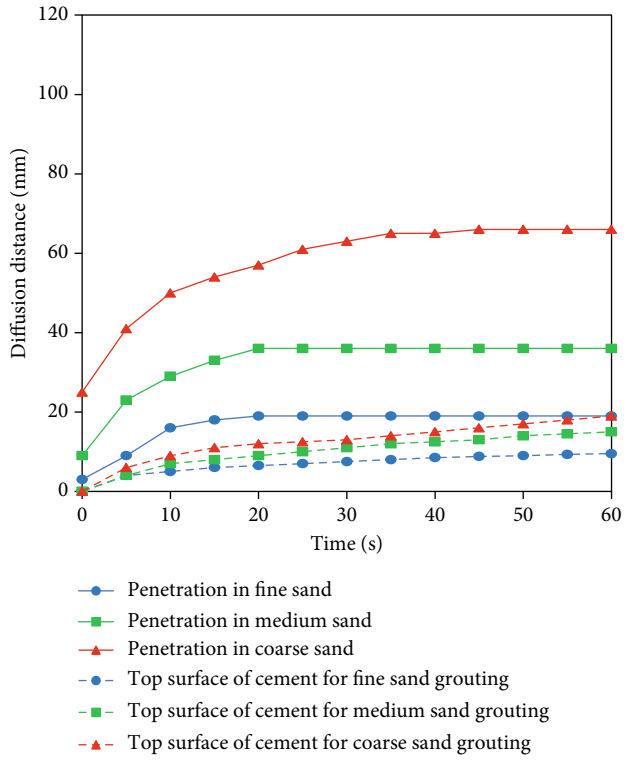

Figure 8: The development of cement farthest penetration surface and the top surface of cement slurry with time (tests 1, 2, and 3).

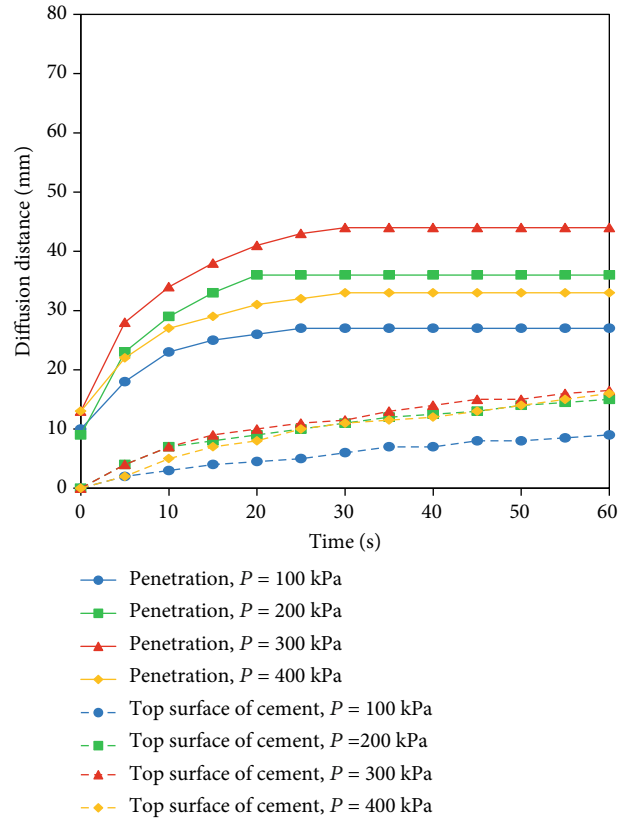

Figure 9: The development of cement farthest penetration surface and the top surface of cement slurry with time (tests 2, 7, 8, and 9).

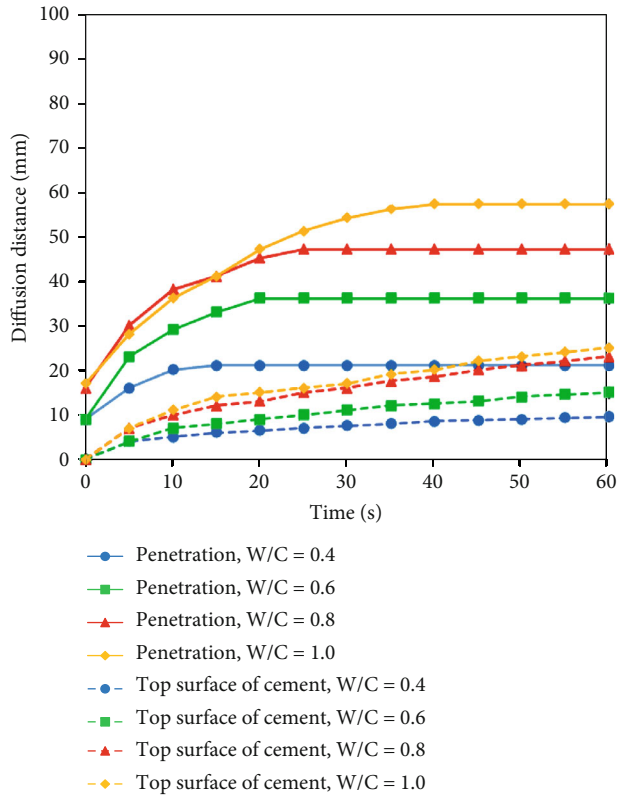

Figure 10: The development of cement farthest penetration surface and the top surface of cement slurry with time (tests 2, 4, 5, and 6).

formation of clogging arch (or named jamming arch), as an arc containing particles can build up in the pore throat which stops the particle flow (the cement particle is smaller than the pore throat). For the latter type of particle clogging, the occurrence of particle clogging at an opening (pore throat) has stochastic property [21–26]. Based on previous studies, the clogging probability is determined by three factors: (a) the solid concentration of the particle flow; (b) the size ratio of the particle to the opening; and (c) the fluid velocity through the opening. These three factors have a coupled effect on the particle clogging probability and the occurrence time of the clogging.

The probability of particle clogging decreases as the solid concentration of the suspension decreases. For cement-based grouting, a higher water-cement ratio means a lower solid concentration of particles. Therefore, particle clogging is less likely to happen as the water-cement ratio increases. Fewer particles are clogged and retained by the pores, and thus, more cement particles can penetrate the soil. Additionally, the clogging probability decreases with increasing the size ratio of opening to the passing particles. Therefore, the cement particles are less likely to become clogged in the pores of the coarse sand column, and the penetration of subsequent particles increases. As for the effect of grouting pressure on filtration, it can be explained from the effect of the passing velocity of particles on the particle clogging.

Mondal et al. [22] and Dai and Grace [23] found that with increasing the flow velocity of the suspension, the clogging probability increases, and the clogging occurs more

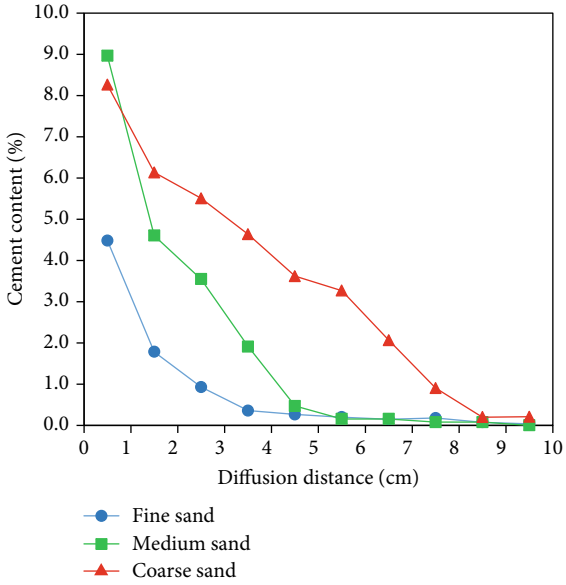

Figure 11: The distribution of penetrated cement content in sand columns (tests 1, 2, and 3).

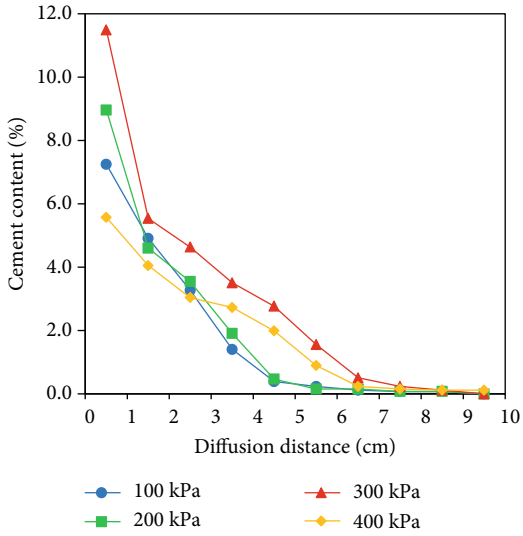

Figure 12: The distribution of penetrated cement content in sand columns (test 2, 7, 8, and 9).

quickly. A higher fluid velocity causes more particles to pass through the opening simultaneously, which is prone to forming the clogging arch. In this work, with the increase of the grouting pressure, the flow velocity of cement slurry increases. More particles pass through the pore throat simultaneously, and thus, more particles are clogged and retained in the pores. Although more cement particles are injected at higher pressure, excessive pressure will accelerate the clogging occurrence and stop the subsequent penetration of cement particles. Thus, the cement penetration distance and amount do not increase monotonously with the growth of the pressure. It is noted that in the laboratory test of Ma et al. [4], the penetration increases monotonously with pressure. It is because the other two factors also influence particle clogging. There is a threshold opening-particle size ratio for the clogging occurrence, which means that regardless of hydraulic grouting conditions, clogging will not occur [23] (particle clogging probability is 0). In this situation, the higher pressure lets more cement particles penetrate the soil without increasing particle clogging. Thus, the cement penetration shows a positive correlation to the grouting pressure.

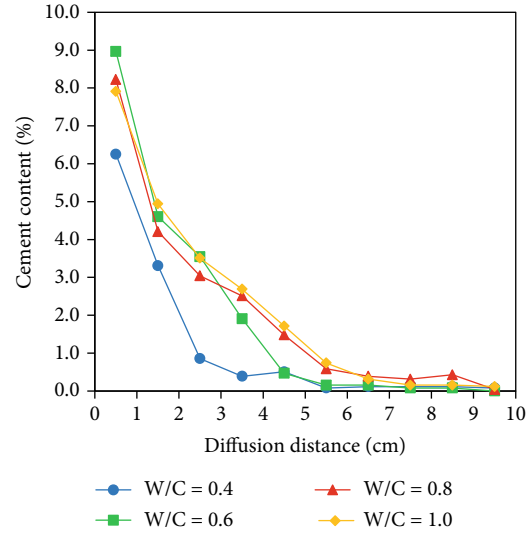

Figure 13: The distribution of penetrated cement content in sand columns (tests 2, 4, 5, and 6).

Once the cement particles eventually clog the soil samples' pores thoroughly, a dense cement cake forms above the soil column (see Figure 18(d)). This cake, also called the filter cake, can be seen as a porous filter constructed by the fine cement particles and the soil particles. It will stop the solid cement particles from penetrating and just allow the water in slurry to pass through. The filter cake is formed at the contact surface between the soil and the slurry because the slurry's velocity and the solid concentration at the contact surface are maximum, which is most conducive to particle clogging.

The formation condition of cement filter cake can be analyzed by the critical opening-particle size ratio for the particle clogging occurrence [15, 23], which means the clogging definitely happens (particle clogging probability is 1) as the opening-particle size ratio is smaller than this value. From the research on the clogging of cement particle [15] in sand, this critical value is 3. In this study, we observed the cement filter cake in all of our grouting tests. The values of b_{K-C}/d_{90} for different soil samples in this work are all smaller than or equal to 3 (see Table 4), which are consistent with the critical value proposed by previous research [15].

4.2. Reduced Permeability of the Soil Column after the Cement Infiltration. From numerous studies dealing with the permeability of sand, the value of permeability coefficient k is determined by the physical properties of the fluid, the soil particles, and the porosity of the packed sands. With the cement particles retained (or called penetrated) in the soil column due to filtration, the porosity and the specific

Table 4: Measured porosity for the different sands and specific surfaces determined from the grain distribution curves.

Sand	Porosity (%)	Specific surface (m^{-1})	b_{K-C} (μm)	b_{K-C}/d_{90}
Coarse	30.3	5538	122	3.0
Medium	35.1	8529	98	2.4
Fine	39.2	15080	66	1.6

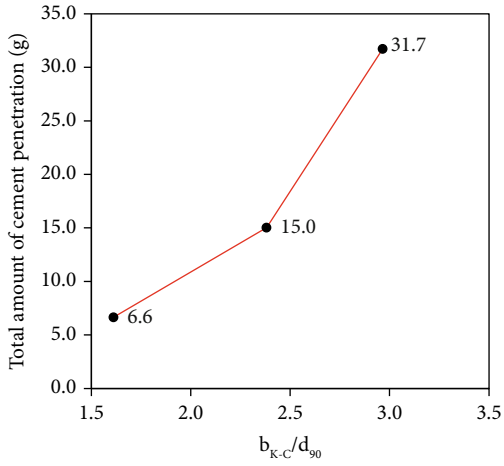

Figure 14: The relationship between b_{K-C}/d_{90} and the total amount of cement penetration.

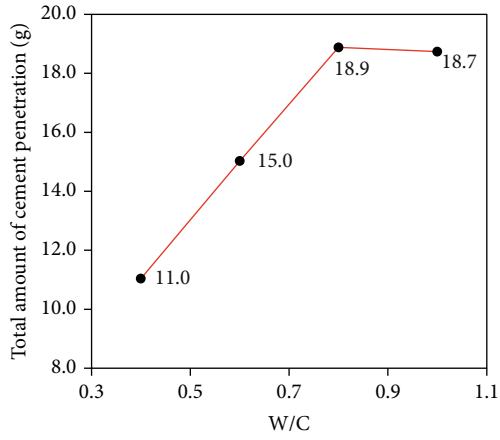

Figure 15: The relationship between W/C and the total amount of cement penetration.

surface area of the soil decrease. Accordingly, the value of the soil column's permeability is reduced. According to widely used Kozeny-Carman function [19], the permeability coefficient k of soil can be calculated by

$$k = \frac{g}{\nu C} \times \frac{1}{S_0^2} \times \frac{n^3}{(1-n)^2}, \quad (4)$$

where S_0 represents the specific surface area, ν is the fluid's kinematic viscosity, and n is the porosity of the soil column. C represents the Kozeny–Carman constant, reported as five

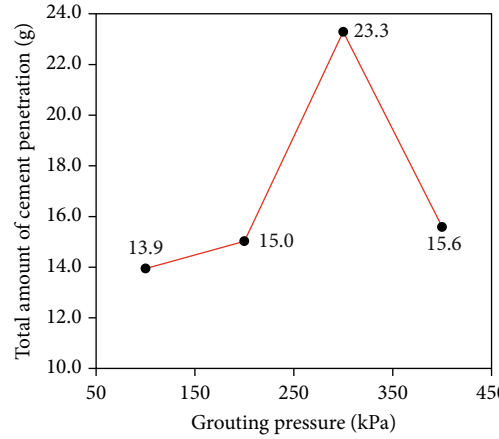

Figure 16: The relationship between grouting pressure and the total amount of cement penetration.

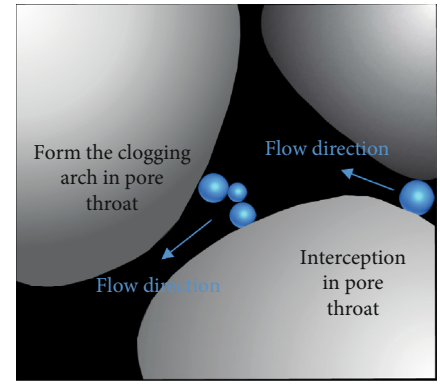

Figure 17: Schematic of two types of particle clogging.

by Zhou et al. [19] for uniform spheres. When the cement particles are retained in the soil column, they become a part of the porous media. The cement particle's specific surface area and the solid volume should be substituted into Equation (4) to calculate the permeability of the soil column after the cement filtration. The dependence of the cement particles on the permeability of the medium-sized soil column utilized in this work is shown in Figure 19.

From this figure, with the increase of the retained cement content in the soil column, the permeability of the soil column k decreases. When cement content is larger than 2%, the permeability of the medium-sized soil column utilized in this work decreases almost exponentially. The value of k with a cement content of 10% is approximately 10^{-3} times that for the clean saturated soil column. The reduced permeability means that the fluid pressure is dramatically lost in the soil column; accordingly, the cement's subsequent penetration rate and distance decrease.

4.3. Dewatering of the Cement Slurry after the Formation of Filter Cake. With continuous grouting, the cement particles clog the soil samples' pores and form a dense cement cake above the soil column (see Figure 18(d)). After the filter cake's formation, the maximum penetration distance of the slurry in soil tends to stabilize. However, the upper surface

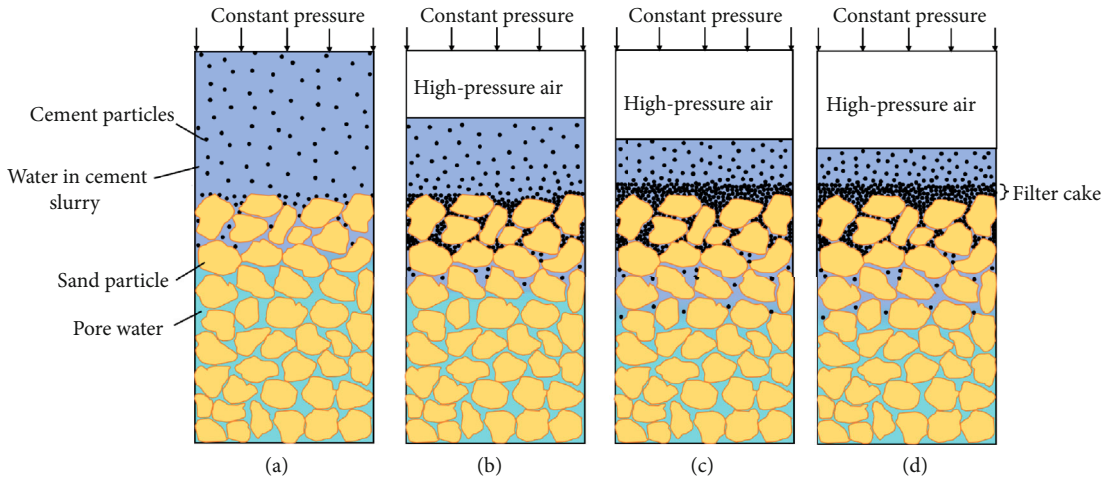

Figure 18: Schematic of the development of the cement penetration, retention into the soil, and the cement filter cake formation above the soil column.

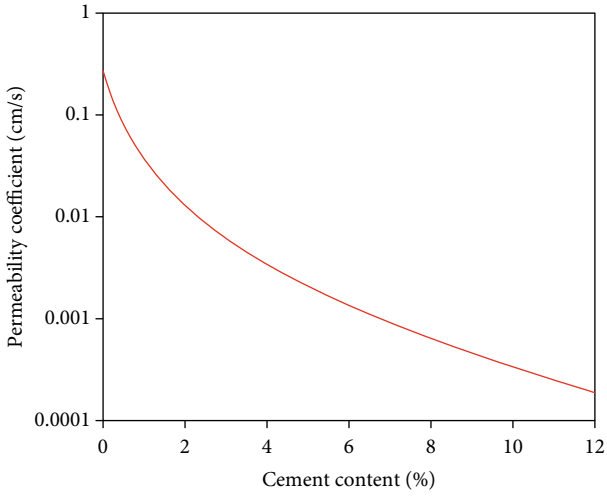

Figure 19: Relationship between cement content and permeability coefficient of medium sand.

of the cement slurry continues to develop gently under the grouting pressure, as shown in Figures 8–10 and sketched in Figures 18(c) and 18(d). That means that the water in cement slurry is drained out (dewatering) because of mass conservation and the incompressibility of the slurry. The formed filter cake stops cement particles' injecting but allows the water in cement-slurry passing through. This phenomenon that slurry is dewatered and thicken above the grouting body after the filter cake formation should be noticed in the grouting design for practical projects.

5. Conclusions

In this study, laboratory tests are conducted to study the filtration of cement-based grouting in saturated sand. By utilizing the visualization grouting device and the ETDA test, the variation of the penetration distance with time and the cement content distribution in the soil column can be measured. The influence of three factors, namely, sand samples' pore size, cement slurry's water-cement ratio, and the value of constant grouting pressure, on the filtration behaviors was discussed in detail. The main conclusions are obtained as follows:

In the case of the same grouting materials, with increasing the ratio size of the pore size to cement particles, the infiltration (or called penetration) depth and the amount increase significantly regardless of the hydraulic grouting conditions.

The cement penetration does not continuously increase with the growth of the grouting pressure. Excessive grouting pressure will accelerate the formation of the filter cake and decrease the subsequent cement particle infiltration.

With the growth of the water-cement ratio, the cement slurry penetration rate and the maximum penetration distance increase continuously. While, in this work, when the water-cement ratio exceeds 0.8, the improvement of the cement penetration by increasing the water-cement ratio is not significant.

The reduced permeability of the soil column because of the cement filtration (retention) was analyzed. When the retained cement content is larger than 2%, the permeability k decreases almost exponentially with the increase of the cement content. The value of k for soil with 10% retained cement content is approximately 10^{-3} times that for the clean saturated soil. In the lower-permeable soil column, fluid pressure loses more, reducing subsequent penetration rates and the distance.

Additionally, pressure filtration of the cement slurry (dewatering and thickening) was observed after the formation of the cement filter cake (see Figure 19). This decreases the effectiveness of cement grouting since subsequent grouting cannot penetrate the soil.

From the viewpoint of particle clogging in the pore throats of the grouting body, the abovementioned grouting parameters determine the probability and occurrence time of particle clogging collectively, leading to different filtration behaviors. More clogging means less penetration, and the filter cake forms more quickly. To alleviate filtration and inject

more cement, particle clogging should be avoided by increasing the size ratio of the pore of the grouting body to cement particles, the water-cement ratio, and choosing an appropriate grouting pressure.

It is noted that the rheological behavior of cement slurry also plays a crucial role in the filtration effect of the cement-based grouts [2, 15]. In this work, the cement slurry does not harden significantly during the short grouting time. Thus, the rheological physics of the cement slurry and its influence on filtration is out of the scope of this work and will be discussed in our future work. The results obtained in this work are helpful to understand the whole filtration process, the mechanism of filtration behaviors, and their deciding factors. Some suggestions are also provided for determining the appropriate grouting parameters for practical grouting projects.

Data Availability

Some or all data, models, or code generated or used during the study are available from the corresponding author by request.

Conflicts of Interest

The authors declare that they have no conflict of interest.

Acknowledgments

This work was supported by the National Natural Science Foundation of China (Grant nos. 52108352, 52078464, and U2006225). The authors are grateful for the above supports.

References

[1] T. Xu and A. Bezuijen, "Experimental study on the mechanisms of bentonite slurry penetration in front of a slurry TBM," *Tunnelling and Underground Space Technology*, vol. 93, article 103052, 2019.

[2] G. Zhu, Q. Zhang, R. Liu, J. Bai, W. Li, and X. Feng, "Experimental and numerical study on the permeation grouting diffusion mechanism considering filtration effects," *Geofluids*, vol. 2021, Article ID 6613990, 11 pages, 2021.

[3] A. Flora, G. Modoni, S. Lirer, and P. Croce, "The diameter of single, double and triple fluid jet grouting columns: prediction method and field trial results," *Géotechnique*, vol. 63, no. 11, pp. 934–945, 2013.

[4] D. Ma, S. Kong, Z. Li, Q. Zhang, Z. Wang, and Z. Zhou, "Effect of wetting-drying cycle on hydraulic and mechanical properties of cemented paste backfill of the recycled solid wastes," *Chemosphere*, vol. 282, article 131163, 2021.

[5] D. Li, X. Li, Y. Hu et al., "Study on dispersion of cement grout in sand considering filtration effect through the EDTA titration test," *Geofluids*, vol. 2020, Article ID 6620979, 9 pages, 2020.

[6] Z. Zhou, H. Zang, S. Wang, X. Du, D. Ma, and J. Zhang, "Filtration behaviour of cement-based grout in porous media," *Transport in Porous Media*, vol. 125, no. 3, pp. 435–463, 2018.

[7] J. S. Dolado and K. van Breugel, "Recent advances in modeling for cementitious materials," *Cement and Concrete Research*, vol. 41, no. 7, pp. 711–726, 2011.

[8] P. Herzig, D. M. Leclerc, and P. L. Goff, "Flow of suspensions through porous media-application to deep filtration," *Industrial and Engineering Chemistry*, vol. 62, no. 5, pp. 8–35, 1970.

[9] T. Krause, *Schildvortrieb mit flüssigkeits-und erdgestützter Ortsbrust*, Mitteilungen des Instituts für Grundbau und Bodenmechanik der Technischen Universität Braunschweig, 1987.

[10] W. Broere, *Tunnel face stability and new CPT applications*, Delft University Press, 2002.

[11] O. S. Q. Yousif, M. Karakouzian, N. O. A. Rahim, and K. A. Rashed, "Physical clogging of uniformly graded porous media under constant flow rates," *Transport in Porous Media*, vol. 120, no. 3, pp. 643–659, 2017.

[12] D. Ma, J. Wang, X. Cai et al., "Effects of height/diameter ratio on failure and damage properties of granite under coupled bending and splitting deformation," *Engineering Fracture Mechanics*, vol. 220, article 106640, 2019.

[13] D. Ma, J. Zhang, H. Duan et al., "Reutilization of gangue wastes in underground backfilling mining: overburden aquifer protection," *Chemosphere*, vol. 264, Part 1, article 128400, 2021.

[14] Z. Zhou, X. Du, S. Wang, X. Cai, and L. Chen, "Micromechanism of the diffusion of cement-based grouts in porous media under two hydraulic operating conditions: constant flow rate and constant pressure," *Acta Geotechnica*, vol. 14, no. 3, pp. 825–841, 2019.

[15] M. Axelsson, G. Gustafson, and Å. Fransson, "Stop mechanism for cementitious grouts at different water-to-cement ratios," *Tunnelling and Underground Space Technology*, vol. 24, no. 4, pp. 390–397, 2009.

[16] F. Bouchelaghem and L. Vulliet, "Mathematical and numerical filtration–advection–dispersion model of miscible grout propagation in saturated porous media," *International Journal for Numerical and Analytical Methods in Geomechanics*, vol. 25, no. 12, pp. 1195–1227, 2001.

[17] Z. Saada, J. Canou, L. Dormieux, J. C. Dupla, and S. Maghous, "Modelling of cement suspension flow in granular porous media," *International Journal for Numerical and Analytical Methods in Geomechanics*, vol. 29, no. 7, pp. 691–711, 2005.

[18] Y. S. Kim and A. J. Whittle, "Particle network model for simulating the filtration of a microfine cement grout in sand," *Journal of Geotechnical and Geoenviromental Engineering*, vol. 135, no. 2, pp. 224–236, 2009.

[19] J. Zhou, K. Fang, and K. Yang, "Bearing capacity of grouted pile considering grout filtration," in *Proceedings of Geo Shanghai 2018 International Conference: Fundamentals of Soil Behaviours*, A. Zhou, J. Tao, X. Gu, and L. Hu, Eds., pp. 645–650, Springer, Singapore, 2018.

[20] P. C. Carman, "Permeability of saturated sands, soils and clays," *The Journal of Agricultural Science*, vol. 29, no. 2, pp. 262–273, 1939.

[21] B. Ahlén, *Effect of cementation and compaction on hydraulic and acoustic properties of porous media*, Chalmers tekniska högskola och Göteborgs universitet, 1993.

[22] S. Mondal, C.-H. Wu, and M. M. Sharma, "Coupled CFD-DEM simulation of hydrodynamic bridging at constrictions," *International Journal of Multiphase Flow*, vol. 84, pp. 245–263, 2016.

[23] J. Dai and J. R. Grace, "Blockage of constrictions by particles in fluid-solid transport," *International Journal of Multiphase Flow*, vol. 36, no. 1, pp. 78–87, 2010.

[24] H. Sun, S. Xu, X. Pan, L. Shi, X. Geng, and Y. Cai, "Investigating the jamming of particles in a three-dimensional fluid-

driven flow via coupled CFD-DEM simulations," *International Journal of Multiphase Flow*, vol. 114, pp. 140–153, 2019.

[25] I. Zuriguel, A. Garcimartin, D. Maza, L. A. Pugnaloni, and J. M. Pastor, "Jamming during the discharge of granular matter from a silo," *Physical Review E*, vol. 71, no. 5, article 051303, 2005.

[26] A. Guariguata, M. A. Pascall, M. W. Gilmer et al., "Jamming of particles in a two-dimensional fluid-driven flow," *Physical Review E*, vol. 86, no. 6, article 061311, 2012.